nature genetics

Prospective functional classification of all possible missense variants in *PPARG*

Amit R Majithia[1–4], Ben Tsuda[1,14], Maura Agostini[5,14], Keerthana Gnanapradeepan[1,14], Robert Rice[1], Gina Peloso[1,6], Kashyap A Patel[7], Xiaolan Zhang[1], Marjoleine F Broekema[8], Nick Patterson[1], Marc Duby[1], Ted Sharpe[1], Eric Kalkhoven[8], Evan D Rosen[4,9], Inês Barroso[5], Sian Ellard[7,10], UK Monogenic Diabetes Consortium[11], Sekar Kathiresan[1,3,4,12], Myocardial Infarction Genetics Consortium[11], Stephen O'Rahilly[5], UK Congenital Lipodystrophy Consortium[11], Krishna Chatterjee[5], Jose C Florez[1–4], Tarjei Mikkelsen[1,13], David B Savage[5,15] & David Altshuler[1–4,13,15]

Clinical exome sequencing routinely identifies missense variants in disease-related genes, but functional characterization is rarely undertaken, leading to diagnostic uncertainty[1,2]. For example, mutations in *PPARG* cause Mendelian lipodystrophy[3,4] and increase risk of type 2 diabetes (T2D)[5]. Although approximately 1 in 500 people harbor missense variants in *PPARG*, most are of unknown consequence. To prospectively characterize PPARγ variants, we used highly parallel oligonucleotide synthesis to construct a library encoding all 9,595 possible single–amino acid substitutions. We developed a pooled functional assay in human macrophages, experimentally evaluated all protein variants, and used the experimental data to train a variant classifier by supervised machine learning. When applied to 55 new missense variants identified in population-based and clinical sequencing, the classifier annotated 6 variants as pathogenic; these were subsequently validated by single-variant assays. Saturation mutagenesis and prospective experimental characterization can support immediate diagnostic interpretation of newly discovered missense variants in disease-related genes.

A major challenge in clinical exome sequencing is determining the pathogenicity of missense variants incidentally found in genes previously implicated in a severe genetic disease[1,2,6]. Every exome contains ~200 missense variants that have never before been seen[7]. Few of these are in fact pathogenic, but functional testing is too slow and resource intensive to be deployed at scale, leading to many variants of uncertain significance (VUS)[8]. The lack of functional data and failure to explicitly incorporate information about ascertainment and prevalence can lead both to misdiagnosis[6,9] (if a benign variant is presumed pathogenic) and overestimation of penetrance (if modestly functional variants are systematically excluded from disease databases).

Peroxisome proliferator–activated receptor γ (PPARγ) exemplifies the challenge of classifying newly identified variants even in a well-studied disease-implicated gene. Rare mutations in *PPARG* cause familial partial lipodystrophy 3 (FPLD3)[3,4], and a common missense variant, p.Pro12Ala, along with linked noncoding variants, associates with risk of T2D[10,11]. The molecular functions of PPARγ are well characterized[12,13], including its role as the target of antidiabetic thiazolidinedione medications. Approximately 0.2% of the general population carries a rare missense variant in *PPARG*, but only 20% of these variants are functionally relevant and associated with metabolic disease[5].

To enable functional interpretation of PPARγ variants identified in exome sequencing, we constructed a cDNA library consisting of all possible amino acid substitutions in the protein (**Fig. 1a** and **Supplementary Fig. 1**). Based on the observation that primary monocytes isolated from the blood of patients with FPLD3 exhibit a blunted PPARγ response when stimulated with agonists *ex vivo*[13], the construct library was introduced into human macrophages edited to lack the endogenous *PPARG* gene (**Supplementary Fig. 2**). After stimulation with PPARγ agonists, cells were sorted by FACS according

[1]Program in Medical and Population Genetics, Broad Institute of Harvard and MIT, Cambridge, Massachusetts, USA. [2]Diabetes Research Center, Diabetes Unit, Department of Medicine, Massachusetts General Hospital, Boston, Massachusetts, USA. [3]Center for Human Genetic Research, Massachusetts General Hospital, Boston, Massachusetts, USA. [4]Department of Medicine, Harvard Medical School, Boston, Massachusetts, USA. [5]University of Cambridge Metabolic Research Laboratories, Wellcome Trust–Medical Research Council Institute of Metabolic Science, Cambridge, UK. [6]Department of Biostatistics, Boston University School of Public Health, Boston, Massachusetts, USA. [7]Institute of Biomedical and Clinical Science, University of Exeter Medical School, Exeter, UK. [8]Molecular Cancer Research and Center for Molecular Medicine, University Medical Centre Utrecht, Utrecht, the Netherlands. [9]Division of Endocrinology and Metabolism, Beth Israel Deaconess Medical Center, Boston, Massachusetts, USA. [10]Department of Molecular Genetics, Royal Devon and Exeter National Health Service Foundation Trust, Exeter, UK. [11]A list of members and affiliations appears in the **Supplementary Note**. [12]Cardiovascular Research Center, Department of Medicine, Massachusetts General Hospital, Boston, Massachusetts, USA. [13]Present addresses: 10X Genomics, Inc., Pleasanton, California, USA (T.M.) and Vertex Pharmaceuticals, Boston, Massachusetts, USA (D.A.). [14]These authors contributed equally to this work. [15]These authors jointly directed this work. Correspondence should be addressed to A.R.M. (amajithia@mgh.harvard.edu).

Received 11 March; accepted 23 September; published online 17 October 2016; doi:10.1038/ng.3700

to the level of expression of CD36, a canonical target of PPARγ in multiple tissues[14,15] (**Fig. 1a**). The sorted CD36$^+$ and CD36$^-$ cell populations were sequenced to determine the distribution of each PPARγ variant in relation to CD36 activity.

'Function scores' were generated for each amino acid substitution at each site in PPARγ (**Figs. 1b** and **2a**, and Online Methods) by partitioning variants into those present in the CD36$^+$ and CD36$^-$ FACS populations. Over 99% of all possible amino acid substitutions in the protein were covered. Of the 20 possible amino acids at each site, a change to proline was most likely to reduce function and a change to cysteine was best tolerated, consistent with the known conformational effects of amino acid side chains on protein structure[16]. Each of the 505 amino acid positions in PPARγ was assigned a 'tolerance score' by combining the function scores for the 19 alternative amino acids at that position (**Fig. 1b**). Tolerance scores were overlaid on the known crystal structure of PPARγ (**Fig. 2b**)[17], demonstrating that amino acid positions that are intolerant of substitution cluster at residues that contact DNA, co-activating proteins, and ligands (rosiglitazone) (**Figs. 1b** and **2b**).

We next examined function scores derived from the CD36 macrophage assay for mutations previously reported in patients with lipodystrophy and/or insulin resistance and known to diminish PPARγ activity (**Fig. 2a**). These pathogenic variants (**Fig. 2a**,**c**) clustered in the PPARγ ligand-binding and DNA-binding domains[4,18] and had function scores demonstrating enrichment in the bin corresponding to 'low' CD36 activity. In contrast, higher-frequency variants, including the common p.Pro12Ala variant, had function scores demonstrating enrichment in the bin corresponding to 'high' CD36 activity (**Fig. 2c** and **Supplementary Table 1**). The distributions of function scores for the pathogenic and common variants were significantly different ($P < 6 \times 10^{-7}$, Kolmogorov–Smirnov test).

We used linear discriminant analysis (LDA) to combine the function scores for each of the 9,595 variants across multiple agonist conditions (**Fig. 2c**) into a classifier that maximized discrimination between the set of lipodystrophy-associated variants and the set of high-frequency variants. The classifier emits the likelihood of each variant being drawn from either of these two classes (pathogenic or benign) and can be expressed as a continuous integrated function score (IFS) (**Fig. 2c**).

As stated above and described in the Online Methods, the classifier was trained on pathogenic variants obtained from the published literature and benign variants from population-based sequencing[19]. To evaluate the performance of the model on independent data, we turned to new variants obtained in population-based exome sequencing and sequencing of *PPARG* in patients referred to specialty clinics for possible lipodystrophy and early-onset diabetes. Specifically, we tested the predictions of functionality emitted by the classifier using standard assays and correlation with clinical phenotypes.

The classifier was applied to data from exome sequencing of 22,106 cases and controls selected for study of early-onset myocardial infarction (MIGEN)[20]. In total, 57 missense variants in *PPARG* were observed with minor allele frequency (MAF) less than 0.1%. Of these, 74% ($n = 42/57$) were new and thus had not previously been functionally characterized (**Supplementary Table 1**). To calculate a posterior probability of pathogenicity relevant to the clinical context in which the carriers were identified, we combined the IFS values for these variants with the estimated prevalence of FPLD3 in the general population (1:100,000 to 1:1,000,000)[18]. One variant, p.Arg194Gln, was estimated to be pathogenic with high posterior odds (benign:pathogenic) of 1:10,000. The individual who was heterozygous for p.Arg194Gln carried a diagnosis of T2D and had fasting triglyceride

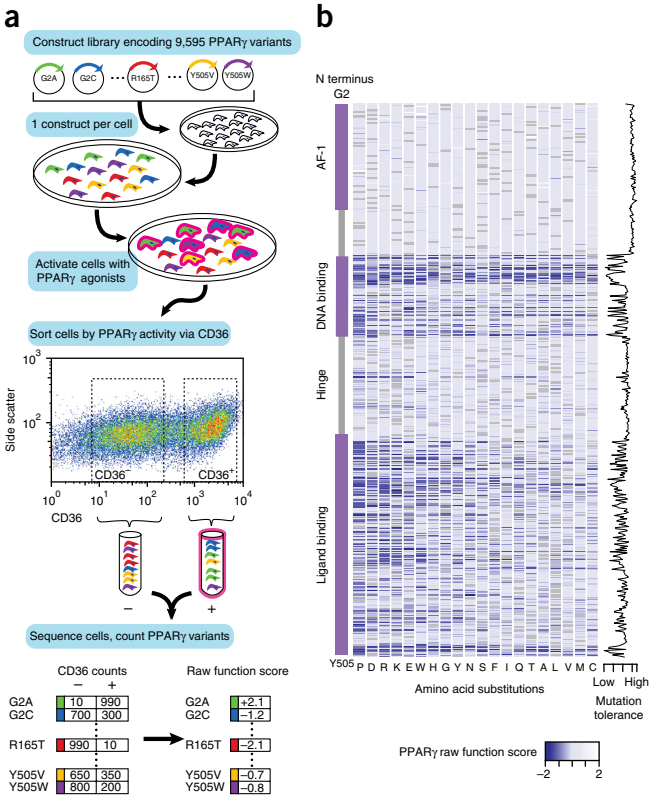

Figure 1 Comprehensive functional testing of 9,595 PPARγ amino acid variants. (**a**) A library of 9,595 *PPARG* constructs was synthesized, with each construct encoding one amino acid substitution. The construct library was introduced into THP-1 monocytes (edited to lack the endogenous *PPARG* gene) such that each cell received a single construct. The polyclonal population of THP-1 monocytes was differentiated into macrophages and stimulated with PPARγ agonists (rosiglitazone and prostaglandin J2), and the stimulated macrophages were separated via FACS according to expression of the PPARγ response gene CD36 into bins with low (–) and high (+) PPARγ activity. Each bin of cells was subjected to next-generation sequencing at the transgenic *PPARG* locus to identify and tabulate the introduced variants. PPARγ variant counts in the bins with low and high CD36 expression were used to calculate a functional score for all 9,595 variants. (**b**) Raw PPARγ function scores for each of the 9,595 variants plotted according to amino acid position along the PPARγ sequence. Blue indicates that an amino acid change away from the reference results in a low CD36 function score, whereas white indicates that a change to the amino acid does not alter function; gray corresponds to the reference amino acid. Function scores summed by amino acid position are plotted to the right, showing the level of tolerance for any amino acid substitution away from the reference.

levels in the 99th percentile (**Supplementary Table 2**). As described below, p.Arg194Gln was independently identified in a separate individual referred for clinical features of lipodystrophy (**Fig. 3** and **Supplementary Table 3**) who similarly manifested T2D and severe hypertriglyceridemia. Moreover, the p.Arg194Gln variant abolished PPARγ transactivation activity in standard assays (**Fig. 3c**). The combination of clinical and functional data indicates that p.Arg194Gln is likely pathogenic and that the individual from MIGEN may have undiagnosed FPLD3.

We next applied the classifier to variants ascertained from 335 patients referred to UK centers specializing in monogenic forms of diabetes and/or insulin resistance. We identified 13 individuals as carrying new missense variants in *PPARG* (**Supplementary Tables 2** and **3**), of whom 77% (10/13) had clinical features suggestive of

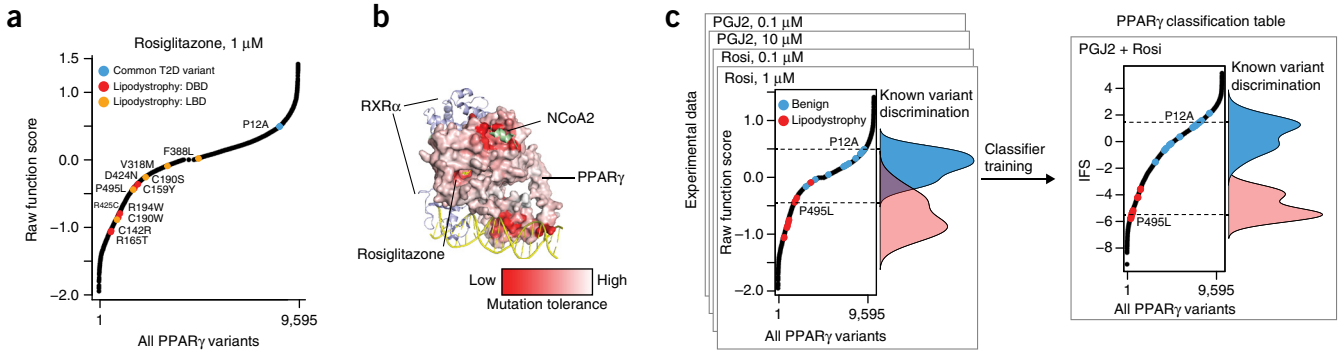

Figure 2 Integrating experimental function to construct a PPARγ classification table. (**a**) Raw PPARγ function scores ranked for all 9,595 PPARγ variants tested. The raw function scores of known lipodystrophy-causing variants are highlighted in red if the variant resides in the DNA-binding domain (DBD) or in orange if it resides in the ligand-binding domain (LBD). The common p.Pro12Ala variant is shown in blue. (**b**) Mutation tolerance scores as described in **Figure 1** are mapped onto the known crystal structure of PPARγ with RXRα, NCoA, and rosiglitazone. Red indicates that the amino acid change away from the reference results in a low CD36 function score, whereas white indicates that the amino acid change does not alter function. (**c**) Raw PPARγ function scores were obtained for 9,595 variants under four experimental conditions: (i) 1 μM rosiglitazone (Rosi); (ii) 0.1 μM rosiglitazone; (iii) 10 μM prostaglandin J2 (PGJ2); and (iv) 0.1 μM prostaglandin J2. The functions of known benign (n = 13) and lipodystrophy-causing (n = 11) variants are highlighted in blue and red, respectively, with their overall distributions overlaid. The raw function scores were combined into an integrated function score (IFS) after classifier training using linear discriminant analysis.

lipodystrophy and associated metabolic derangement, including severe insulin resistance, non-alcoholic fatty liver, dyslipidemia, and low serum adiponectin levels (**Supplementary Table 3**). The IFS values for these 13 variants were lower than those found in the population-based cohort ($P < 0.005$, Student's t test) (**Fig. 3a**). For each variant, the posterior probability of pathogenicity was calculated by combining the IFS for that variant and the prevalence of FPLD3 in patients ascertained in these specialty clinics (~1:7, as estimated from Cambridge national lipodystrophy clinic records).

We found three variants (p.Glu54Gln, p.Asp92Asn, and p.Asp230Asn) in patients without clinical features of lipodystrophy who had been referred for sequencing on the basis of suspected monogenic diabetes. Despite having a higher prior probability because of their ascertainment in specialty clinics, these three variants were classified as benign with high confidence (posterior odds (benign: pathogenic) = 200:1) (**Supplementary Table 2**). Moreover, when tested individually in standard PPARγ reporter assays, the corresponding mutants showed function indistinguishable from that of wild-type PPARγ (**Fig. 3c**). Thus, the rate of benign variant identification in individuals ascertained in specialty clinics (~1:110, n = 335) was similar to the rate of benign variants identified in the MIGEN cohort (~1:200, n = 22,106).

Three variants (p.Met31Leu, p.Arg308Pro, and p.Arg385Gln) classified as benign with high confidence were found in individuals with clinical features of partial lipodystrophy. The p.Met31Leu variant was found in a female proband with features of lipodystrophy and metabolic derangement (**Supplementary Table 3**); critically, her daughter had a very similar fat distribution and metabolic phenotype

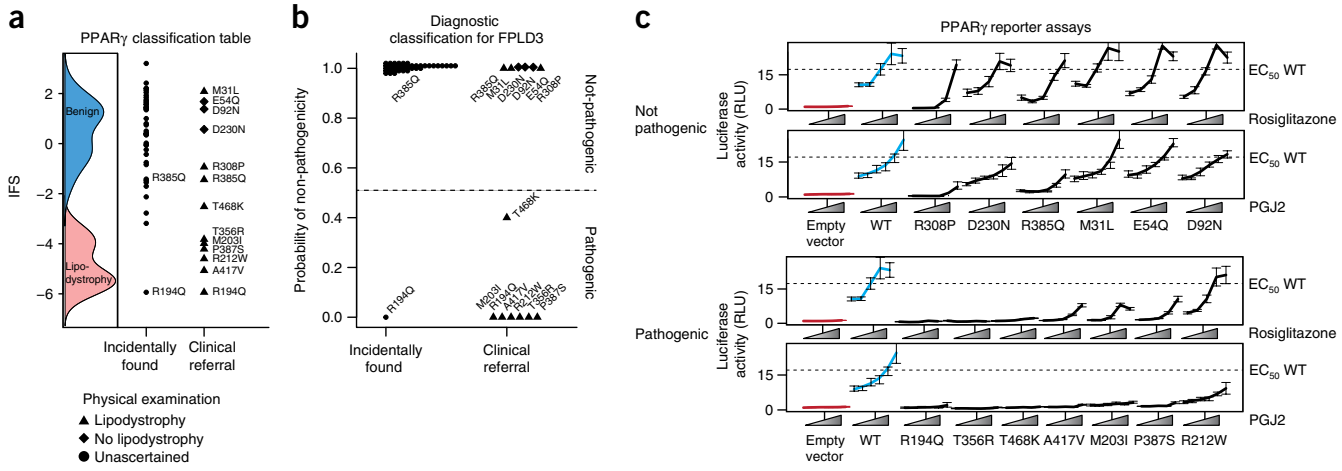

Figure 3 Experimental and clinical classification of new missense *PPARG* variants identified in sequenced individuals. (**a**) Variants identified in subjects plotted according to IFS alongside the IFS distributions of known benign and lipodystrophy-associated variants. (**b**) Diagnostic classification for FPLD3 expressed as the posterior probability of non-pathogenicity for the PPARγ variants shown in **a**. Posterior probability was calculated by combining IFS values with the prevalence of lipodystrophy in the general population (1:100,000) or in patients referred for lipodystrophy or familial diabetes (1:7). (**c**) The variants identified in subjects were individually recreated and tested for their ability to activate luciferase reporter constructs containing three copies in tandem of the PPRE from the *ACOX1* gene (acyl-CoA oxidase) linked to the thymidine kinase promoter under varying doses of pharmacological (rosiglitazone) or endogenous (prostaglandin J2) ligand. Data are shown as means ± s.e.m.; n = 5. Variants are grouped according to their non-pathogenic/pathogenic designations in **b**. RLU, relative luciferase units; WT, wild type; EC_{50}, half-maximal effective concentration.

but did not carry the p.Met31Leu variant. Thus, in this case, the phenotype did not segregate with genotype at *PPARG*. An individual with partial lipodystrophy carried a p.Arg385Gln variant, which was independently identified in a woman from the population-based cohort who had not developed T2D by age 61 years (**Supplementary Table 2**). When tested in PPARγ reporter assays, corresponding mutants retained reporter activity, albeit their activity was subtly diminished under some conditions (**Fig. 3**). The combination of functional testing, clinical data, segregation, and epidemiological analysis suggests that p.Met31Leu, p.Arg308Pro, and p.Arg385Gln are likely incidental findings, although it is not possible to rule out the possibility that they act as partial risk factors for metabolic phenotypes.

Six variants (p.Arg194Gln, p.Ala417Val, p.Arg212Trp, p.Pro387Ser, p.Met203Ile, and p.Thr356Arg) were found in patients with lipodystrophy and classified as pathogenic with high probability (posterior odds (benign:pathogenic) = 1:>25,000). Five of the six were confirmed to result in defective protein in classical transactivation assays. The exception was p.Arg212Trp, for which the corresponding mutant protein had normal transactivation function when tested using a synthetic PPARγ response element (PPRE). However, Arg212Trp showed less activity than wild-type PPARγ in a reporter assay with an endogenous promoter (**Fig. 4a**) and reduced *in vitro* binding to three PPREs (**Fig. 4b**). The Arg212 side chain forms multiple hydrogen-bond contacts in the minor groove of DNA (**Fig. 4c**), outside the main PPRE binding motif. These data indicate that p.Arg212Trp is likely a pathogenic variant despite it not resulting in decreased activity in the traditional functional assay using a synthetic promoter.

Finally, p.Thr468Lys, found in a single patient with partial lipodystrophy, was classified by IFS as pathogenic with low confidence (posterior odds (benign:pathogenic) = 2:3); its score fell in the overlapping tails of the distributions for benign and lipodystrophy-associated variants. In PPARγ reporter assays, this variant resulted in severely decreased function (**Fig. 3**), supporting the view that p.Thr468Lys is likely a pathogenic variant.

We previously reported that rare missense variants in *PPARG* that impair function in a single-variant adipocyte differentiation assay confer increased risk of T2D in the general population[5]. We reexamined this relationship using functional annotation emitted by the classifier (that is, IFS values) for the original sample of 118 *PPARG* variant carriers ascertained from 19,752 T2D cases and controls (**Fig. 5a**). We observed a long tail of variants with low IFS in T2D cases but not controls ($P = 0.024$, two-sample Kolmogorov–Smirnov test). We quantified this inverse relationship between IFS and T2D case status (logistic regression $\beta = -0.49 \pm 0.15$ (standard error), $P = 0.002$). The odds ratio for T2D in carriers of variants with the lowest tertile of IFS values (as compared to carriers of variants with IFS values in the highest tertile) was 6.5 (95% confidence interval (CI) = 1.9–41), consistent with our previously published estimate[5]. The odds ratio for the middle versus highest tertile of IFS values was 2.0 (95% CI = 1.3–3.1), suggesting that PPARγ variants with even moderately reduced IFS confer a modest increase in T2D risk. By contrast, a conventional predictor of mutation deleteriousness (CONDEL score[21]) failed to distinguish between likely pathogenic and benign variants ($P > 0.1$, two-sample Kolmogorov–Smirnov test; **Fig. 5b**), misclassifying many likely benign variants as pathogenic (**Fig. 5c**).

These data show that it is possible to experimentally characterize all possible missense variants in a mammalian gene and use the information to guide interpretation of variants of uncertain significance, a concept that has previously been applied to single protein domains[22,23]. Testing variants prospectively (that is, before their discovery in patients) overcomes barriers of time and scalability

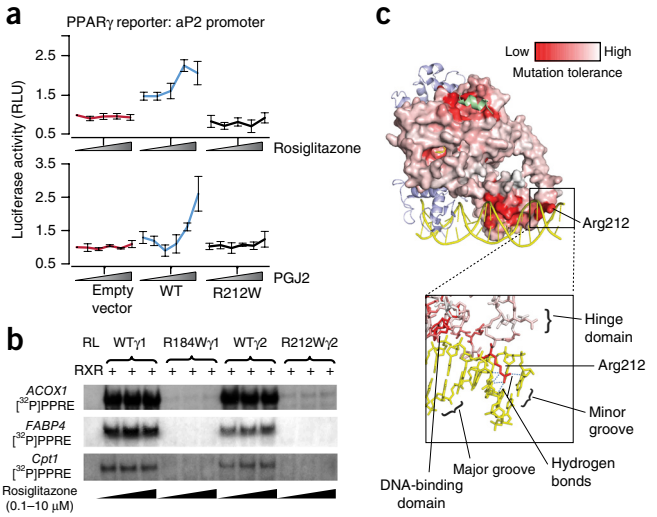

Figure 4 Ability of the PPARγ Arg212Trp variant to transactivate gene expression and bind DNA at endogenous enhancers. (**a**) Ability of wild-type PPARγ and the Arg212Trp mutant to activate luciferase reporter constructs containing the *FABP4* (aP2) promoter under varying doses of pharmacological (rosiglitazone; 0–1 μM) or endogenous (prostaglandin J2; 0–10 μM) ligand. Data are shown as means ± s.e.m; $n = 5$. (**b**) Comparison of the DNA-binding properties of *in vitro*–translated wild-type and mutant PPARγ proteins, tested in electrophoretic mobility shift assays using either isoform 1 (γ1; Arg184Trp) or isoform 2 (γ2; Arg212Trp) mutants and radiolabeled PPREs from the human *ACOX1* (5′-GGACCAGGACAAAGGTCACGTT-3′), human *FABP4* (5′-AAACACAGGCAAAGGTCAGAGG-3′), and mouse *Cpt1* (5′-ATCGGTGACCTTTTCCCTACA-3′) promoters with retinoid X receptor (RXR) and increasing concentrations of ligand (rosiglitazone; 0–10 μM).RL, reticulocyte lysate. (**c**) PPARγ residues colored by mutation tolerance scores obtained under stimulation with 1 μM rosiglitazone in THP-1 cells. As in **Figure 2b**, red indicates sites that exhibited low CD36 response when mutated away from the wild-type residue. Arg212 is highlighted; it occurs in the 'hinge' region of PPARγ connecting the DNA-binding and ligand-binding domains. The positively charged arginine side chain extends into the minor groove of DNA, forming multiple hydrogen bonds with bases.

that have thus far made it impractical to incorporate experimental data into routine clinical variant interpretation. Furthermore, by simultaneously and consistently evaluating all variants in a single experiment, more valid comparisons can be made across variants as compared to data on different variants generated in different laboratories at different times.

The *PPARG* classifier annotated as benign nearly all variants (56/57) incidentally identified in a study of myocardial infarction. The one variant classified as pathogenic with high confidence (and confirmed by single-variant laboratory experiments) was observed in an individual with hypertriglyceridemia and T2D and was independently observed in a patient with lipodystrophy, likely indicating FPLD3 (ref. 24). In 12 of 13 cases referred for suspected lipodystrophy or monogenic diabetes and carrying a *PPARG* variant, the classifier provided immediate, high-confidence information regarding the likelihood of a functional defect and a molecular diagnosis of FPLD3. In only a single case (p.Thr468Lys) did the classifier not provide a high-confidence estimate and low-throughput laboratory assays fail to corroborate the pooled assay data[13].

Systematic variant construction, pooled experimental characterization in relevant assays, and statistical integration with epidemiological data offers a generalizable approach to enable genome interpretation

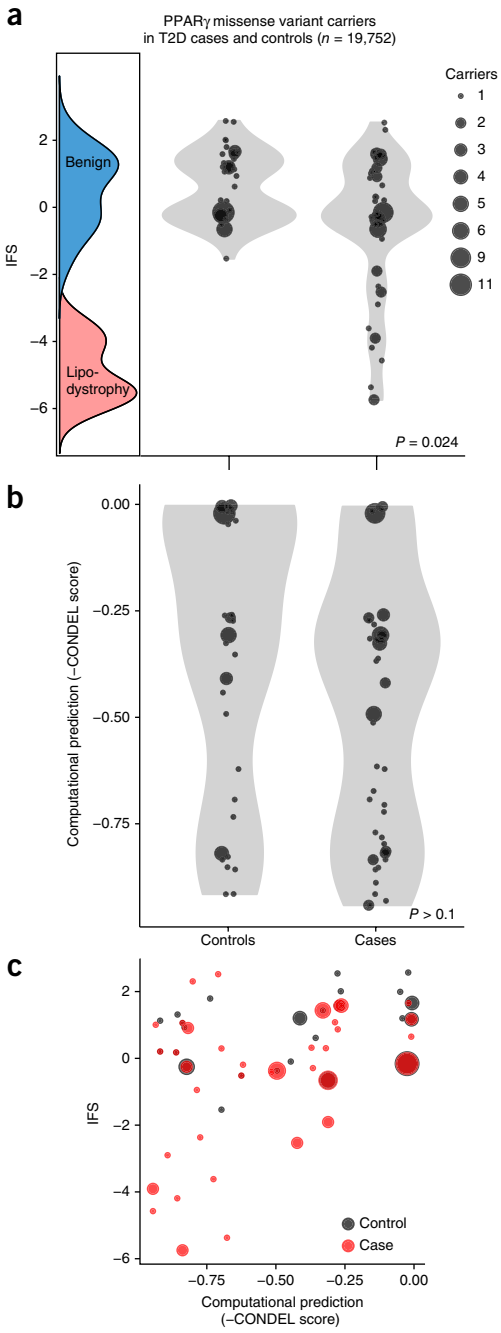

Figure 5 Relationship of PPARγ function to T2D risk in the general population. (**a**) Missense PPARγ variants identified from 19,752 sequenced T2D cases and controls plotted according to IFS from the PPARγ classification table alongside the IFS distributions of known benign and lipodystrophy-associated variants. Each point represents a missense variant; point size corresponds to the number of individuals carrying that variant. Among the 118 individuals carrying missense PPARγ variants, T2D cases contained a long tail of missense variants resulting in low function, which was notably absent from the distribution of variants observed in T2D controls ($P = 0.024$, two-sample Kolmogorov–Smirnov test). (**b**) When variants from the same 118 individuals were plotted according to computational prediction of deleteriousness (CONDEL score), no difference in the distribution of functional variants is seen between T2D cases and controls ($P > 0.1$, two-sample Kolmogorov–Smirnov test). (**c**) Scatterplot of computational prediction score versus IFS for PPARγ missense variants from T2D cases and controls.

at clinically important genes, reducing overdiagnosis[6,9] and diagnostic uncertainty[8]. Fully realizing such comprehensive approaches will require a complementary array of methods[25]. The *PPARG* construct library is easily shared so that others can generate and contribute function scores in other assays[26], but as a transgene library it is not ideally suited for detecting the functional effects of coding variation on splicing efficiency. Given the limitations on the library and because CD36 expression is unlikely to report on all the functions of PPARγ, we have made the *PPARG* classifier available as a web application (MITER; see URLs) that can be updated as new genetic and functional data become available. Broadening this approach to other genes and diseases will require cellular assays that are disease relevant, robust, and scalable, and will also depend on the availability of training sets of pathogenic and benign variants. Such assays and variants exist for a number of genes implicated in Mendelian disease, making it possible to apply a similar approach to help interpret variants of uncertain significance for many other clinical situations.

URLs. MITER, http://miter.broadinstitute.org/; National Severe Insulin Resistance Service, http://www.cuh.org.uk/national-severe-insulin-resistance-service; Diabetes Genes, http://www.diabetesgenes.org/; lentivirus protocols, http://portals.broadinstitute.org/gpp/public/resources/protocols; cell lines, http://www.broadinstitute.org/achilles.

METHODS

Methods and any associated references are available in the online version of the paper.

Note: Any Supplementary Information and Source Data files are available in the online version of the paper.

ACKNOWLEDGMENTS

This work was supported by grants from the National Institute of Diabetes and Digestive and Kidney Diseases (1K08DK102877-01, to A.R.M.; 1R01DK097768-01, to D.A.), NIH/Harvard Catalyst (1KL2TR001100-01, to A.R.M.), the Broad Institute (SPARC award, to A.R.M. and T.M.), and the Wellcome Trust (095564, to K.C.; 107064, to D.B.S.).

We thank J. Doench, C. Zhu, D. O'Connell, G. Cowley, M. Sullender, D. MacArthur, E. Minkel, B. Bulik-Sullivan, and J. Avruch for helpful discussions, laboratory assistance, and manuscript review.

This paper is dedicated to the memory of Promila Nandi (30 April 1933–27 December 2013).

AUTHOR CONTRIBUTIONS

A.R.M., T.M., and D.A. designed the study. A.R.M., B.T., M.A., and K.G. performed experiments with help from R.R., X.Z., M.F.B., and E.K. A.R.M. and N.P. analyzed the data with help from B.T., T.S., G.P., K.A.P., M.D., and T.M. I.B., S.E., S.K., S.O'R., K.C., and D.B.S. contributed clinical data and genotypes. A.R.M. and D.A. wrote the manuscript. D.B.S., S.O'R., K.C., E.D.R., and J.C.F. revised the manuscript.

COMPETING FINANCIAL INTERESTS

The authors declare no competing financial interests.

1. Majewski, J., Schwartzentruber, J., Lalonde, E., Montpetit, A. & Jabado, N. What can exome sequencing do for you? *J. Med. Genet.* **48**, 580–589 (2011).
2. Gahl, W.A. *et al.* The National Institutes of Health Undiagnosed Diseases Program: insights into rare diseases. *Genet. Med.* **14**, 51–59 (2012).
3. Barroso, I. *et al.* Dominant negative mutations in human PPARγ associated with severe insulin resistance, diabetes mellitus and hypertension. *Nature* **402**, 880–883 (1999).
4. Jeninga, E.H., Gurnell, M. & Kalkhoven, E. Functional implications of genetic variation in human PPARγ. *Trends Endocrinol. Metab.* **20**, 380–387 (2009).
5. Majithia, A.R. *et al.* Rare variants in *PPARG* with decreased activity in adipocyte differentiation are associated with increased risk of type 2 diabetes. *Proc. Natl. Acad. Sci. USA* **111**, 13127–13132 (2014).

6. Flannick, J. *et al.* Assessing the phenotypic effects in the general population of rare variants in genes for a dominant Mendelian form of diabetes. *Nat. Genet.* **45**, 1380–1385 (2013).
7. Tennessen, J.A. *et al.* Evolution and functional impact of rare coding variation from deep sequencing of human exomes. *Science* **337**, 64–69 (2012).
8. McLaughlin, H.M. *et al.* A systematic approach to the reporting of medically relevant findings from whole genome sequencing. *BMC Med. Genet.* **15**, 134 (2014).
9. Manrai, A.K. *et al.* Genetic misdiagnoses and the potential for health disparities. *N. Engl. J. Med.* **375**, 655–665 (2016).
10. Altshuler, D. *et al.* The common PPARγ Pro12Ala polymorphism is associated with decreased risk of type 2 diabetes. *Nat. Genet.* **26**, 76–80 (2000).
11. Claussnitzer, M. *et al.* Leveraging cross-species transcription factor binding site patterns: from diabetes risk loci to disease mechanisms. *Cell* **156**, 343–358 (2014).
12. Tontonoz, P. & Spiegelman, B.M. Fat and beyond: the diverse biology of PPARγ. *Annu. Rev. Biochem.* **77**, 289–312 (2008).
13. Agostini, M. *et al.* Non–DNA binding, dominant-negative, human PPARγ mutations cause lipodystrophic insulin resistance. *Cell Metab.* **4**, 303–311 (2006).
14. Yu, S. *et al.* Adipocyte-specific gene expression and adipogenic steatosis in the mouse liver due to peroxisome proliferator–activated receptor γ1 (PPARγ1) overexpression. *J. Biol. Chem.* **278**, 498–505 (2003).
15. Tontonoz, P., Nagy, L., Alvarez, J.G., Thomazy, V.A. & Evans, R.M. PPARγ promotes monocyte/macrophage differentiation and uptake of oxidized LDL. *Cell* **93**, 241–252 (1998).
16. Barnes, M.R. & Gray, I.C. *Bioinformatics for Geneticists* (Wiley, 2003).
17. Chandra, V. *et al.* Structure of the intact PPAR-γ–RXR-α nuclear receptor complex on DNA. *Nature* **456**, 350–356 (2008).
18. Garg, A. Acquired and inherited lipodystrophies. *N. Engl. J. Med.* **350**, 1220–1234 (2004).
19. Lek, M. *et al.* Analysis of protein-coding genetic variation in 60,706 humans. *Nature* **536**, 285–291 (2016).
20. Myocardial Infarction Genetics Consortium Investigators. *et al.* Inactivating mutations in *NPC1L1* and protection from coronary heart disease. *N. Engl. J. Med.* **371**, 2072–2082 (2014).
21. González-Pérez, A. & López-Bigas, N. Improving the assessment of the outcome of nonsynonymous SNVs with a consensus deleteriousness score, Condel. *Am. J. Hum. Genet.* **88**, 440–449 (2011).
22. Fowler, D.M. *et al.* High-resolution mapping of protein sequence–function relationships. *Nat. Methods* **7**, 741–746 (2010).
23. Starita, L.M. *et al.* Massively parallel functional analysis of BRCA1 RING domain variants. *Genetics* **200**, 413–422 (2015).
24. Demir, T. *et al.* Familial partial lipodystrophy linked to a novel peroxisome proliferator activator receptor-γ (*PPARG*) mutation, H449L: a comparison of people with this mutation and those with classic codon 482 Lamin A/C (*LMNA*) mutations. *Diabet. Med.* **33**, 1445–1450 (2016).
25. Findlay, G.M., Boyle, E.A., Hause, R.J., Klein, J.C. & Shendure, J. Saturation editing of genomic regions by multiplex homology-directed repair. *Nature* **513**, 120–123 (2014).
26. Fowler, D.M. & Fields, S. Deep mutational scanning: a new style of protein science. *Nat. Methods* **11**, 801–807 (2014).

ONLINE METHODS

Synthesis and assembly of 9,595 *PPARG* variant constructs. A library of all 9,595 possible single–amino acid variants in PPARγ was synthesized using a site-directed, multiplexed method (Mutagenesis by Integrated TilEs (MITE); ref. 27) adapted to render it suitable for saturation mutagenesis in mammalian cells. Detail is provided below where methodological advancements were made to permit saturation mutagenesis of *PPARG*. First, the *PPARG* cDNA sequence (CCDS2609.1) was recoded (**Supplementary Table 4**) to eliminate susceptibility to restriction enzymes and CRISPR/Cas9 targeting sgRNAs to enable a 'delete-and-replace' strategy. As described previously, DNA oligonucleotides were synthesized on a programmable microarray, with each oligonucleotide encoding a desired amino acid change but otherwise homologous to the template, unmutated *PPARG* sequence in all other respects. Oligonucleotides were organized into 'tiles', with those within each tile differing in a central variable region but having identical 5′ and 3′ ends (**Supplementary Table 4**). Tiles were staggered such that their variable regions collectively spanned the entire template. To ensure uniform amplification and reduce chimera formation for the longer *PPARG* template, the protocol was modified to amplify each tile by emulsion PCR (MICELLULA DNA Emulsion and Purification Kit, EURx). The resulting products were inserted into linearized plasmids (Phusion High-Fidelity DNA Polymerase; NEB, M0530) that carried the remaining template sequence using multiplexed Gibson assembly (NEBuilder HiFi DNA Assembly Master Mix; NEB, E2621L) according to the manufacturer's protocol. A 'frameshift-cleaning' procedure was introduced given that the most common error mode during library construction (25–30% of constructs; data not shown) resulted from oligonucleotide synthesis errors causing 1- to 2-bp indels. The *PPARG* template vector was designed such that all *PPARG* constructs terminated with amber stop codons (TAG) and bore an in-frame zeocin resistance cassette (pUC57-PPARG-zeo; GenScript). Constructs bearing frame-shifting indels were depleted by transformation into an amber suppressor cloning host (TG1, Lucigen) and dual selection of the construct library with zeocin and kanamycin. Library plasmids were purified from $>10^6$ colonies to preserve complexity, and the frameshift-depleted *PPARG* transgenes were excised from the zeocin resistance cassette. To enable mammalian cell transduction, the transgene library was transferred into a lentiviral expression vector by simple restriction cloning and transfected into a packaging cell line to produce pooled lentivirus according to standard protocols (pLXI_TRC401; see URLs)[5].

Deletion of endogenous *PPARG* in THP-1 monocytes using CRISPR/Cas9. The endonuclease Cas9 and sgRNAs targeting exon 6 of *PPARG* and exon 8 of a control gene, *PHACTR1*, were introduced into THP-1 cells by lentiviral transduction (**Supplementary Table 4**). To quantify modification of the endogenous gene, genomic DNA was extracted at multiple time points, amplified by PCR around the *PPARG* sgRNA target site and Sanger sequenced (**Supplementary Table 4**). Cutting efficiency was determined using the TIDE web tool for decomposition analysis of the sequencing traces[28]. Twenty-one days after transduction of CRISPR/Cas9 with *PPARG* or control sgRNAs, cells were tested for PPARγ response by gene (*FABP4*) and protein (CD36) expression to validate lack of functional endogenous PPARγ. THP-1 cells treated with *PPARG*-targeting sgRNA and control sgRNA were stimulated with 1 μM rosiglitazone in THP-1 growth medium (RPMI-1640 supplemented with 10% FBS and 1% penicillin-streptomycin) for 72 h. mRNA was then extracted and quantified for *FABP4* gene expression (nanoString Technologies). For CD36 protein expression, THP-1 cells were stimulated with 50 ng/ml phorbol ester (PMA) and 1 μM rosiglitazone in growth medium for 72 h. Cells were then detached from the plate, washed and stained with a monoclonal antibody to CD36 according to the manufacturer's protocol (Miltenyi, 130-100-149) and subjected to flow cytometry.

Simultaneous testing of 9,595 *PPARG* variants in experimental assays. The *PPARG* construct library was introduced into a human monocytic cell line (THP-1; obtained from the Broad Institute and tested negative for mycoplasma; see URLs) engineered through CRISPR/Cas9 to lack endogenous *PPARG* (**Supplementary Fig. 2**) by pooled infection. While isoform 1 of *PPARG* is dominantly expressed in monocytes and macrophages, we expressed isoform 2, which is identical in sequence but encodes a protein with an additional 28 N-terminal amino acids. Both isoforms demonstrated identical ligand-dependent activity. Pooled virus was diluted such that the multiplicity of infection (number of viral particles per cell) was 0.3 so that each monocyte would receive zero or a single *PPARG* variant. Uninfected cells were eliminated by selection with 2 μg/ml puromycin. Expression of the *PPARG* transgene was controlled by a doxycycline-inducible promoter[5]. At least 1×10^7 cells were infected to ensure that each *PPARG* variant was independently represented in 1,000 monocytes. The resulting polyclonal population of THP-1 monocytes containing the *PPARG* variant library was stimulated for 72 h with (i) 50 μM PMA to induce differentiation into macrophages; (ii) 1 μg/ml doxycycline to induce expression of *PPARG* constructs; and (iii) a low or high dose (based on ranges used in previous studies[13]) of thiazolidinedione (rosiglitazone; 0.1–1 μM) or proposed natural ligand[29] (prostaglandin J2; 0.1–10 μM) to stimulate PPARγ activity. The population of stimulated THP-1 macrophages was immunostained for CD36 (Miltenyi, 130-095-472), a cell surface protein that is a direct transcriptional target of PPARγ[15]. Using FACS, stained cells were grouped into two activity bins separated by at least five- to tenfold difference in expression of CD36 and selected to encompass equal numbers of cells (**Supplementary Fig. 3**). For each stimulation condition, at least three replicates were generated, each with at least 5×10^6 cells sorted. To again identify and quantify the *PPARG* variants in the bins with high and low CD36, genomic DNA was extracted from the cells in each bin and the integrated proviral *PPARG* transgene was amplified by PCR and shotgun sequenced (Nextera, Illumina). Raw sequencing reads were aligned to the reference *PPARG* cDNA sequence (**Supplementary Table 4**), and the number of occurrences of each amino acid at each position along the coding region was counted and tabulated with a custom aligner. To minimize erroneous mutation calls, only codons that matched designed mutations and consisted of high-quality base calls (Phred score >30) were tabulated. Over 99% of the designed amino acid substitutions were observed at least 50 times for a given experimental condition (**Supplementary Fig. 1**). A raw function score was calculated on the basis of the ratio of observed frequencies of each mutant amino acid in the two CD36 activity bins (**Fig. 1**).

Calculation of raw function score. Control experiments showed that variants deleterious to PPARγ function were enriched in the fraction with low CD36 and benign variants were enriched in the fraction with high CD36. We constructed a likelihood function based on the log odds of an amino acid variant being in the fraction with high or low CD36. The log odds for each amino acid variant was estimated by maximizing a likelihood function based on the observed counts of each amino acid variant in the fractions with high and low CD36 as well as the total read depth at that amino acid position. Data were combined across experimental replicates after determining replicate variability (**Supplementary Fig. 4**). To avoid spuriously high or low log-odds estimates for any given variant, we constrained the log-odds estimate with a Gaussian prior whose parameters were estimated from data combined across all variants (see the **Supplementary Note** for detailed specification of the analytical methods used).

Construction of a *PPARG* classifier by supervised machine learning. To predict the likelihood of new variants being benign or pathogenic, we developed a classifier based on raw function scores obtained across various experimental conditions. The synthesis of multiple experimental conditions was intended to span a greater range of possible activities of PPARγ than would be queried using a single condition. Specifically, we used LDA (MASS package in R 3.0) to train the classifier, adopting a two-class model. The model incorporates as parameters (i) raw function scores for each PPARγ variant as measured across the four experimental conditions (rosiglitazone and prostaglandin J2 at high and low doses) and (ii) mutation tolerance scores calculated for each position in PPARγ as measured across the four experimental conditions (**Fig. 1b**). Potential classifiers were systematically constructed on linear combinations of four of these eight parameters, with a requirement that one parameter be included from each experimental condition. Classifier models were built for each of the 16 possible combinations of 4 parameters using a training set of pathogenic and benign PPARγ variants (**Supplementary Table 1**). Pathogenic variants used to train the classifier were selected on the basis of (i) segregation with FPLD3 and (ii) previous demonstration of loss of function in cellular

doi:10.1038/ng.3700

assays. Benign variants used to train the classifier were selected from among variants identified in 60,706 aggregated exome sequences[19] at an allele frequency rendering them very unlikely to be causal for FPLD3 under a dominant model of inheritance and a prevalence estimate ranging from 1:100,000 to 1:1,000,000 ($P < 0.05$, one-tailed binomial probability, $n = 121{,}412$ chromosomes; $P = 1 \times 10^{-5}$) (**Supplementary Table 1**). The performance of these 16 models was compared using a leave-one-out cross-validation (LOOCV) protocol with each model scored by its aggregate ability to correctly classify the 'left-out' variant over all the cycles of LOOCV. The highest scoring model consisted of raw function scores for each possible variant obtained from three conditions (1 μM rosiglitazone, 0.1 μM rosiglitazone, 10 μM prostaglandin) and mutation tolerance scores for each position in *PPARG* obtained under treatment with 0.1 μM prostaglandin. This model was fit to the full training data set for prospective evaluation of new *PPARG* variants. The weighted sum of the four parameters in the final model, as fit by the LDA algorithm, is denoted as the IFS (**Fig. 2c** and **Supplementary Fig. 5**) and represents an aggregate measure of variant function over the four experimental conditions. For clinical prediction, the IFS was expressed as the odds (benign:pathogenic), which when multiplied by the estimated prior odds of FPLD3 based on the clinical situation (prevalence) yielded an estimated probability of pathogenicity. Because the final model was trained on the full set of available pathogenic and benign variants, its performance next required prospective evaluation on a completely independent set of variants. These variants were obtained from the population and clinic data described below and were evaluated as described in **Figure 3**.

Missense *PPARG* variants identified in population-based exomes and clinically referred individuals. The study was conducted in accordance with the Declaration of Helsinki, and approved by research ethics committees; written informed consent was obtained from all participants.

Missense *PPARG* variants were extracted from 22,106 exomes (8,400 with early-onset coronary artery disease and 12,804 controls) sequenced by the Myocardial Genetics Consortium (MIGEN) as described elsewhere[20]. Study participants were ascertained from the following studies: ATVB, DHM, DUKE, JHS, ESP-EOMI, MedStar, OHS, PennCath, PROCARDIS, PROMIS, and REGICOR. Participants were of European ancestry ($n = 12{,}849$; 58%), Asian ancestry ($n = 6{,}823$; 31%), African ancestry ($n = 2{,}399$; 11%), and 'other or unknown' self-reported ancestry ($n = 34$; 0.2%). Twenty-two percent ($n = 4{,}258$) reported a diagnosis of T2D.

Patients were referred to one of two UK centers (Cambridge or Exeter; see URLs) that specialize in syndromes of severe insulin resistance and/or monogenic forms of diabetes. In clinically suspected FPLD3 cases, mutations in *PPARG* were identified in genomic DNA extracted from peripheral blood leukocytes using *PPARG* amplification and sequencing. In patients for whom FPLD3 was not the primary clinical diagnosis, *PPARG* was sequenced as part of a targeted next-generation panel of 29 genes[30] selected to improve diagnostic yield for suspected monogenic diabetes. Variants were confirmed in index patients and, where possible, family members. In all instances, the nomenclature used for missense variants is for isoform 2 of *PPARG* (transcript NM_015869.4; protein NP_056953.2).

Individual testing of *PPARG* variant function by transcriptional activity. The new variants identified in patients with suspected familial lipodystrophy or diabetes were characterized using a well-established PPARγ reporter containing three copies in tandem of the PPRE from *ACOX1* (5′-GGACCAGGACAAAGGTCACGTT-3′) upstream of the thymidine kinase (TK) promoter and luciferase. In brief, 293EBNA cells, cultured in DMEM supplemented with 10% FCS, were transfected with Lipofectamine 2000 in 24-well plates and assayed for luciferase and β-galactosidase activity as described previously[13] following 36 h of incubation with or without ligand.

27. Melnikov, A., Rogov, P., Wang, L., Gnirke, A. & Mikkelsen, T.S. Comprehensive mutational scanning of a kinase *in vivo* reveals substrate-dependent fitness landscapes. *Nucleic Acids Res.* **42**, e112 (2014).
28. Brinkman, E.K., Chen, T., Amendola, M. & van Steensel, B. Easy quantitative assessment of genome editing by sequence trace decomposition. *Nucleic Acids Res.* **42**, e168 (2014).
29. Forman, B.M. *et al.* 15-deoxy-δ12,14-prostaglandin J2 is a ligand for the adipocyte determination factor PPARγ. *Cell* **83**, 803–812 (1995).
30. Ellard, S. *et al.* Improved genetic testing for monogenic diabetes using targeted next-generation sequencing. *Diabetologia* **56**, 1958–1963 (2013).